metals

MDPI

Article

Rare Earth Metal Ion-Associates in Ln^{3+}—CO_3^{2-}—H_2O System

Tatiana Litvinova [1], Stepan Gerasev [2,*], Vasiliy Sergeev [1] and Egor Lidanovskiy [3]

[1] The Department of General and Physical Chemistry, Empress Catherine II Saint Petersburg Mining University, 199106 Saint Petersburg, Russia; litvinova_te@pers.spmi.ru (T.L.); sergev_vv2@pers.spmi.ru (V.S.)
[2] The Metallurgy Department, Empress Catherine II Saint Petersburg Mining University, 199106 Saint Petersburg, Russia
[3] The Department of Chemical Engineering and Energy Processing, Empress Catherine II Saint Petersburg Mining University, 199106 Saint Petersburg, Russia; s220186@stud.spmi.ru
* Correspondence: s235035@stud.spmi.ru

Abstract: This study focused on the nature of rare earth metal complex compounds that can form during the carbonate–alkaline processing of industrial waste materials, such as phosphogypsum and red mud, at 70–100 °C and 1–10 atm. Experimental findings revealed that the dissolution of synthetic carbonates of rare earth elements (REEs) in a concentrated carbonate-ion medium (3 mol/L) leads to the formation of ion-associates of varying strengths. Light (lanthanum, praseodymium, and neodymium) and medium (samarium) REE groups exhibited a tendency to form loose ion-associates, whereas heavy REEs (terbium, dysprosium, holmium, erbium, thulium, lutetium, and yttrium) formed close ion-associates. To confirm the existence of these ion-associates, the specific conductivity of solutions was measured after dissolving thulium (III) and samarium (III) carbonates at phase ratios ranging from 1:2000 g/mL to 1:40 g/mL in a potassium carbonate medium. The decay of ion-associates, leading to the precipitation of rare earth metal (III) carbonates, was tested in an ammonium carbonate medium. Thermal decomposition of ammonium carbonate at 70–75 °C during 1–4 h was accompanied by full rare earth carbonates' sedimentation and its in-the-way separation into groups because of the varied strength of ion-associates. The results of this study provide a basis for developing processes to separate rare earth metals into groups during their carbonate–alkaline extraction into solution.

Keywords: rare earth metals; lanthanides; ion-associates; carbonate complexes; rare earth carbonates; solubility; ammonium carbonate; potassium carbonate

check for updates

Academic Editors: Ilhwan Park and Sanghee Jeon

Received: 23 January 2025
Revised: 19 February 2025
Accepted: 22 February 2025
Published: 24 February 2025

Citation: Litvinova, T.; Gerasev, S.; Sergeev, V.; Lidanovskiy, E. Rare Earth Metal Ion-Associates in Ln^{3+}—CO_3^{2-}—H_2O System. *Metals* **2025**, *15*, 239. https://doi.org/10.3390/met15030239

Copyright: © 2025 by the authors. Licensee MDPI, Basel, Switzerland. This article is an open access article distributed under the terms and conditions of the Creative Commons Attribution (CC BY) license (https://creativecommons.org/licenses/by/4.0/).

1. Introduction

Rare earth metals (REMs) are among the key types of strategic mineral resources, comprising 17 elements: 15 lanthanides, yttrium, and scandium [1–3]. The unique physicochemical properties of REMs enable their use in the production of permanent magnets, batteries, lasers, construction materials, alloys, catalysts, optical glasses, and various other products and intermediates. These materials are particularly essential in military industries, mechanical engineering, and medicine [4–6].

Among the existing classifications of REMs, the following are the most widely applied: [7,8]:

1. By Mass
   - Light (La–Nd);
   - Medium (Sm–Gd);
   - Heavy (Dy–Lu, Y).

2. By Importance, to eliminate the disbalance between global production and consumption of individual REEs
   - Critical (Nd, Eu, Tb, Dy, Er, Y);
   - Non-critical (La, Pr, Sm, Gd, Lu);
   - Surplus (Ce, Ho, Tm, Yb).

Monazite, xenotime, bastnasite, loparite, and other minerals serve as natural sources of surplus, non-critical, and critical REMs alike [9–11]. However, the generation of significant amounts of REM-containing industrial waste, such as phosphogypsum (PG) and red mud (RM), has made the recycling of secondary raw materials increasingly important [12–14]. Globally, PG reserves are estimated at 7–8 billion tons, while RM exceeds 4 billion tons, with REM content in these materials up to 0.9% [15–17].

Although the extraction of REMs and their compounds from traditional sources is predominantly achieved through acid-based methods, the processes developed over the past decades for processing PG and RM using mineral acids lack sufficient economic and/or environmental efficiency [18–20]. In this regard, the alternative carbonate–alkaline method—treatment with ammonium carbonate or alkali metal carbonate solutions—best meets modern requirements. However, it still requires optimization in terms of REMs' extraction into solution and their subsequent separation [21,22].

The development of technical solutions for REM recovery remains constrained by the lack of definitive data on the forms of lanthanides, scandium, and yttrium in a carbonate-ion medium. Exceptions include a limited number of studies, such as those by Millero [23], Byrne [24], and others.

It is known that REMs in PG and RM can exist in the form of various sparingly soluble compounds: fluorides, sulfates, and phosphates in PG, and hydroxides and carbonates in RM [25,26]. REM cations (Ln^{3+}), as well as the corresponding precipitates, are capable of forming carbonate complexes of variable composition, $Ln(CO_3)_n^{3-2n}$, under the influence of an excess of carbonate ions. However, the structures of the resulting compounds remains uncertain [27–29].

On the one hand, the interaction of Ln^{3+} with CO_3^{2-} (1) may involve the formation of classical coordination compounds, consisting of a central Ln ion and CO_3^{2-} ligands. Under standard conditions, for $n = 1$, the stability constant K_1 ranges from 6.52 to 9.15, and for $n = 2$ K_2 it ranges from 11.58 to 17.41 [30–32]. Stability constants are presented in Table 1. On the other hand, the presence of a stability constant alone does not provide definitive evidence of a coordination compound.

Table 1. Stability constants of REM carbonate complexes [32].

REM	Ohta and Kawabe		Liu and Burne		REM	Ohta and Kawabe		Liu and Burne	
	lgK_1	lgK_2	lgK_1	lgK_2		lgK_1	lgK_2	lgK_1	lgK_2
La	8.33	12.52	6.52	11.58	Dy	8.95	14.38	7.33	13.18
Ce	8.58	13.06	6.86	12.05	Ho	8.96	14.48	7.32	13.27
Pr	8.73	13.43	7.03	12.37	Er	9.02	14.62	7.38	13.39
Nd	8.75	13.59	7.08	12.46	Tm	9.10	14.79	7.45	13.54
Sm	8.90	13.95	7.25	12.82	Yb	9.15	14.94	7.58	13.56
Eu	8.86	14.02	7.26	12.91	Lu	9.13	14.96	7.53	13.64
Gd	8.78	13.95	7.17	12.76	Y	8.88	14.29	7.25	12.90
Tb	8.88	14.22	7.23	13.05	Sc	-	17.41	-	-

Moreover, the nature of the bond between a REM ion and a carbonate anion remains unclear. Some researchers [33,34] suggest the possible formation of a complex in the form of an ion-associate (Figure 1), as follows:

$$Ln^{3+}_{(aq)} + nCO^{2-}_{3(aq)} \rightarrow Ln(CO_3)^{3-2n}_{n(aq)} \quad (1)$$

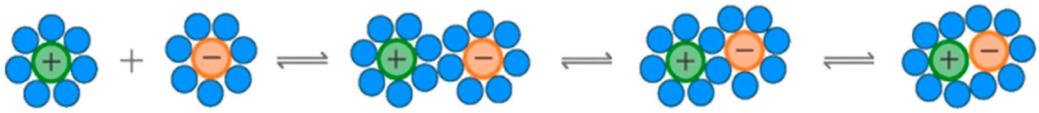

Figure 1. Mechanism of contact (close) ion pair formation [33].

These forms are composed of particles held together by electrostatic attraction forces and comply with Coulomb's law. Such behavior of lanthanides has been confirmed, for instance, for Yb^{3+} and Lu^{3+} ions in a Cl^- medium at concentrations exceeding 2 mol/L [34–36].

Thermodynamic evidence for the formation of ion pairs, triplets, and other structures lies in the high positive entropy values associated with the formation of ion-associates [33]. Due to the limited availability of literature data on the thermodynamics of the association processes involving REM cations and carbonate anions, the most analogous association process is (2), where the entropy of associate formation under standard conditions is 83 ± 12 J/(mol·K) [37]:

$$CaCO_{3(s)} + CO^{2-}_{3(aq)} \rightarrow Ca(CO_3)^{2-}_{2(aq)} \quad (2)$$

The entropy of formation for REM carbonate complexes under standard conditions, calculated using the Latimer–Powell equation, ranges from 159.9 J/(mol·K) to 266.9 J/(mol·K), which theoretically confirms the formation of $Ln(CO_3)_n{}^{3-2n}$ as an ion-associate [38].

According to the literature, the formation of ion-associates in solution does not lead to changes in its conductivity. Ion pairing or association occurs when oppositely charged ions are closer than a certain critical distance. They then can act as a neutral form and hence do not contribute to conductivity [34,39].

Based on the above, determining the type of soluble REM form in a carbonate-ion medium facilitates the development of approaches for their subsequent extraction and separation from the productive solution. Therefore, the aim of this study was to establish the feasibility of REM ion-associates existing in the Ln^{3+}—$CO_3{}^{2-}$—H_2O system.

2. Materials and Methods

Measuring the specific electrical conductivity (SEC) of the system formed during the dissolution of synthetic REM (III) carbonates in a potassium carbonate medium facilitated confirming or refuting the presence of associates.

The use of $Ln_2(CO_3)_3$ as the material for conductometric studies eliminated the influence of foreign anions and/or added water on SEC values. The selected concentration of the potassium carbonate solution, 3 mol/L, corresponded to the range in which SEC increases with concentration (Figure 2) and remained within the sensitivity limits of the device («Anion 4100»). The main technical characteristics of «Anion 4100» are its measurement range of SEC from 10^{-6} S/cm to 10^{-1} S/cm and that its limit of permissible basic relative SEC measurement error of solutions is no more than 2%.

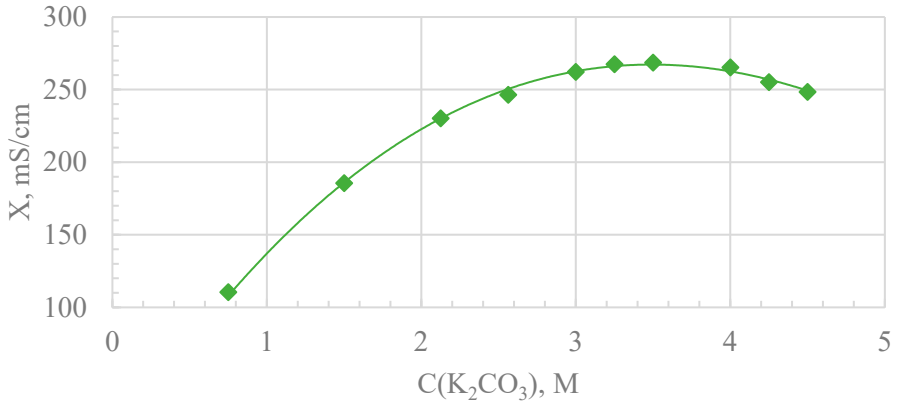

Figure 2. Dependence of solution-specific electrical conductivity on K_2CO_3 concentration at 25 °C.

This study of the effect of potassium, sodium, and ammonium cations on REM carbonate solubility in 0.5–3 M of carbonate ion medium was undertaken using cerium carbonate as an example under standard conditions and a liquid-to-solid ratio of 2000 mL/g (Figure 3).

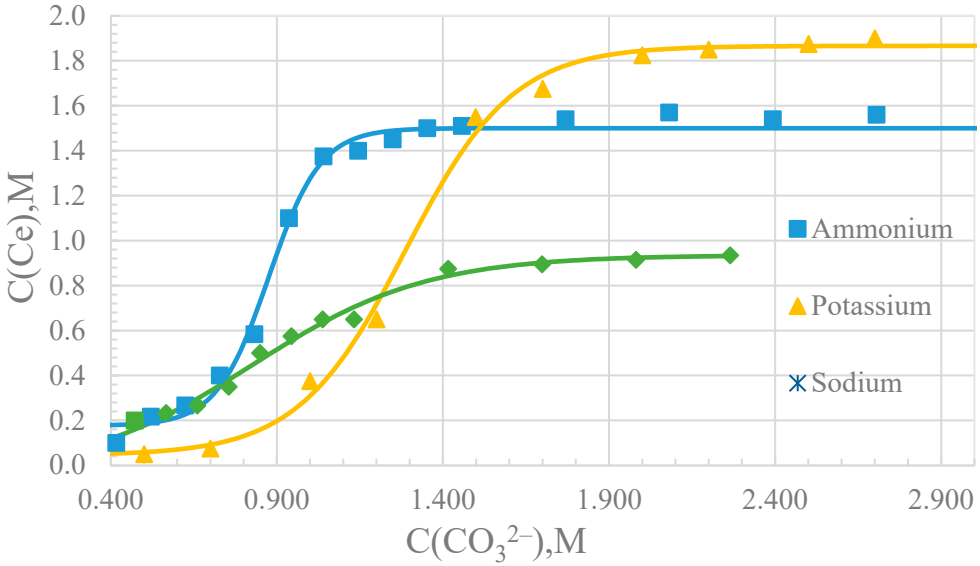

Figure 3. Influence of carbonate ion concentration on cerium (III) carbonate solubility at 25 °C.

The main laboratory equipment for all declared experiments was a HEL Automate II Parallel Reactor System (H.E.L. Group, London, UK) fitted with temperature and stirring speed sensors. Thus, the mixtures' mixing was organized thermostatically.

This series of experiments was conducted under standard conditions by mixing solid REM (III) carbonate with a potassium carbonate solution at solid-to-liquid ratios from 1:2000 g/mL to 1:40 g/mL. Each experiment was carried out for 12 h with stirring at 200 rpm to reach an equilibrium characterized by the complete dissolution of the precipitate.

Another potential method for identifying the soluble forms of REMs is monitoring the reduction in carbonate ion concentration after the complexation process. When a complex ion, $Ln(CO_3)_n^{3-2n}$, is formed via covalent bonds, a decrease in CO_3^{2-} concentration does not lead to its decay due to the relatively high stability constants. In contrast, the presence of ion-associates would result in their decomposition, as ion pairs and other associates are prone to it [40]. As among soluble carbonates only ammonium carbonate tends to decompose at temperatures below the boiling point of the solution (60–70 °C), the reduction in concentration due to thermal decomposition was studied in this medium. In this series

of experiments, solutions of REM nitrate (0.4 mol/L) and ammonium carbonate (3 M) were mixed during 5–10 min at a volume ratio of 1:20 mL/mL. After precipitation and subsequent dissolution, the solution was heated to 70–75 °C. The secondary precipitate formed during ammonium carbonate decomposition was quantified using a gravimetric method, while the REM concentration in the final solution was determined via complexometric titration with Trilon B in the presence of Arsenazo (III) using Equation (3):

$$C_{Ln} = \frac{C_{TB} \times V_{TB}}{V_{Ln}} \quad (3)$$

where C_{Ln}—normal concentration of REM (III), eq/L; V_{Ln}—volume of the aliquot, L; C_{TB}—normal concentration of Trilon B (III), eq/L; and V_{TB}—volume of the titrant, L.

Among the possible insoluble REM (III) compounds that could form upon the decay of the ion-associate, only $Ln_2(CO_3)_3$ was considered. For precipitates obtained, identification was determined via SEM-EDX analysis by scanning electron microscope VEGA 3 LMH with an energy dispersive X-ray microanalysis system (TESCAN Essence, Brno, Czech Republic). Thus, the REM carbonate yield can be calculated using Equation (4):

$$\eta_{Ln_2(CO_3)_3} = \frac{m^p_{Ln_2(CO_3)_3}}{m^t_{Ln_2(CO_3)_3}} \times 100\% = \frac{m^p_{Ln_2(CO_3)_3} \times 2}{C_{Ln(NO_3)_3} \times V_{Ln(NO_3)_3} \times M_{Ln_2(CO_3)_3}} \times 100\% \quad (4)$$

where $\eta_{Ln_2(CO_3)_3}$—yield of $Ln_2(CO_3)_3$, %; $m^p_{Ln_2(CO_3)_3}$—the mass of $Ln_2(CO_3)_3$ after drying, g; $m^t_{Ln_2(CO_3)_3}$—stoichiometrically calculated mass of $Ln_2(CO_3)_3$, g; $C_{Ln(NO_3)_3}$—the concentration of the $Ln(NO_3)_3$, solution, mol/L; $V_{Ln(NO_3)_3}$—the volume of the $Ln(NO_3)_3$, solution, L; and $M_{Ln_2(CO_3)_3}$—the molar mass of $Ln_2(CO_3)_3$.

The concentration of ammonium carbonate in the final solution was determined using conductometric titration with sodium hydroxide.

A short thermodynamic assessment of performed processes was completed. The Gibbs energy change during these reactions to REM carbonates obtained through its ion-associates was estimated by applying the Hess law. A database of the Chemistry Faculty of Moscow State University «https://www.chem.msu.ru/cgi-bin/tkv.pl» (accessed on 17 February 2025) was chiefly used for this purpose.

3. Results

The experimentally determined SEC of the aqueous potassium carbonate solution at 25 °C was 263.2 mS/cm. Upon adding a sample of thulium (III) carbonate to this solution at solid-to-liquid ratios of 1:2000 g/mL, 1:100 g/mL, and 1:40 g/mL, the electrical conductivity of the system decreased, reaching a minimum 2 min after mixing. The conductivity values were 259.1 mS/cm, 253.1 mS/cm, and 252.2 mS/cm, respectively. Whereafter, they gradually returned to the initial conductivity value of 263.2 mS/cm by 4, 6, and 9 min (Figure 4).

The yields of REM (III) carbonates were calculated after heating the solutions that contained the rare earth metals (III) ion-associates for 60, 120, and 240 min (Figure 5), as follows:

1. Yield of $Ln_2(CO_3)_3$ after 60 min: La—98.8 %; Nd—98.3 %; Pr—99.6 %; Sm—97.9 %; Tb—99.4 %; Dy—87.2 %; Ho—63.3 %; Y (Er)—51.6 %; Tm—0 %; Lu—0 %.
2. Yield of $Ln_2(CO_3)_3$ after 120 min: La—98.8 %; Nd—98.3 %; Pr—99.6 %; Sm—97.9 %; Tb—99.4 %; Dy—98.4 %; Ho—74.5 %; Y (Er)—60.9 %; Tm—5 %; Lu—5 %.
3. Yield of $Ln_2(CO_3)_3$ at 240 min reached approximately 100 %, including Tm and Lu.

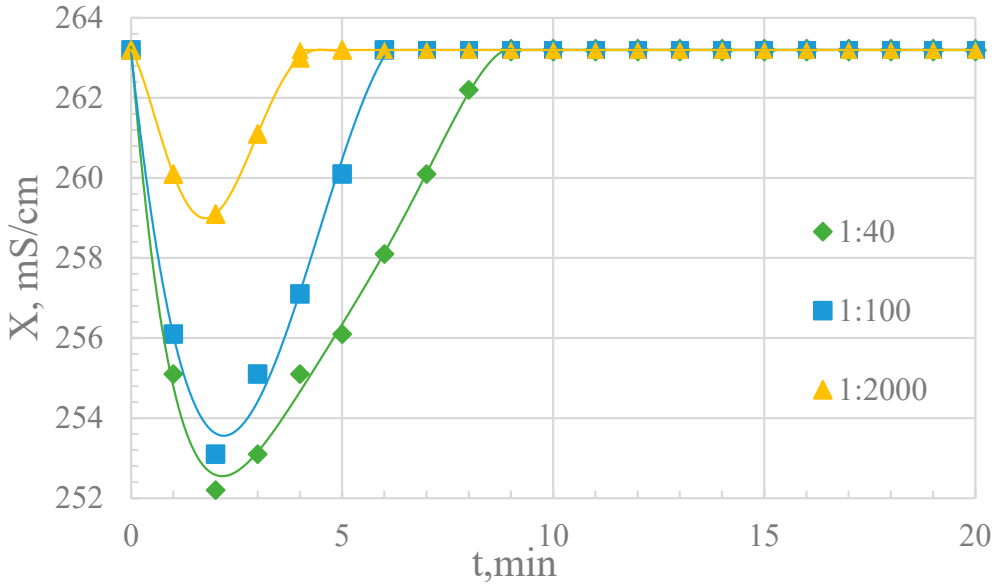

Figure 4. Change in specific electrical conductivity upon adding $Tm_2(CO_3)_3$ to K_2CO_3 solution.

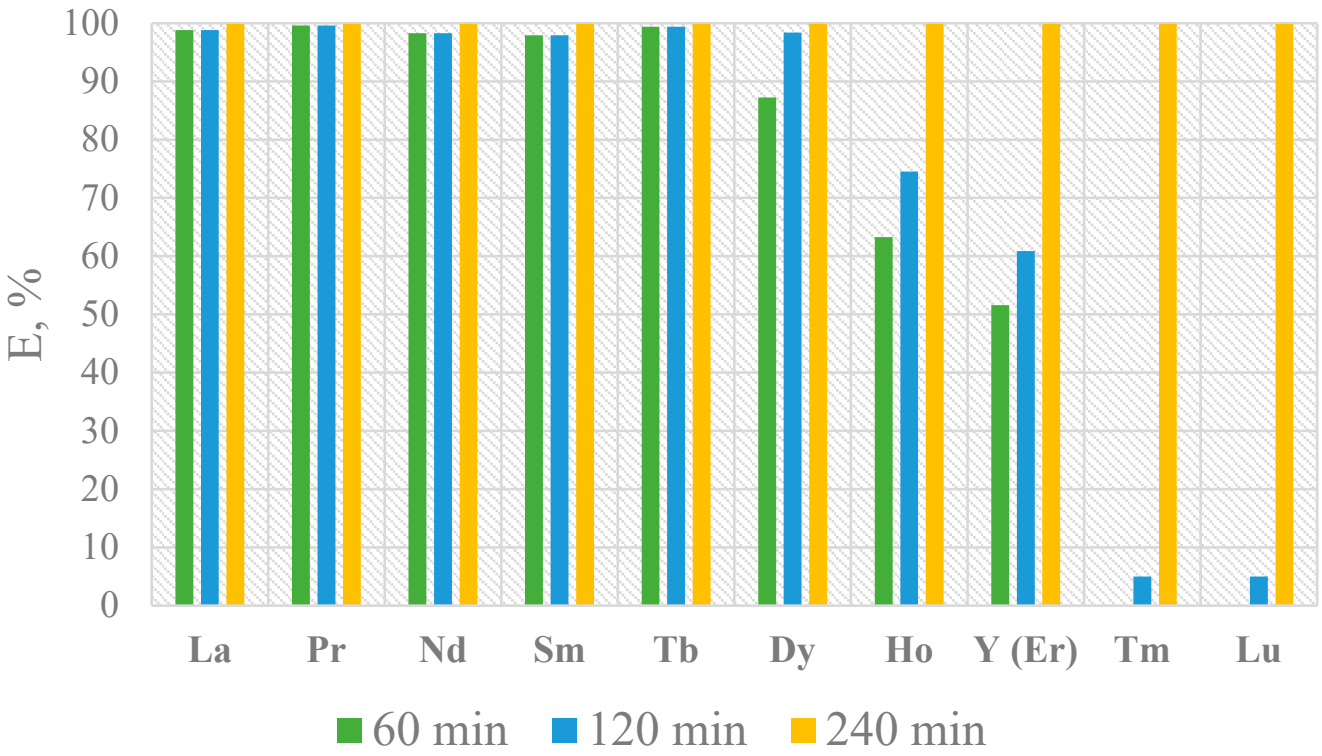

Figure 5. Yield of $Ln_2(CO_3)_3$ upon decay of ion-associates.

The kinetics of ammonium carbonate decomposition were studied using a model solution (initial concentration 3 mol/L) at a temperature of 70–75 °C over a period of 3 h. Based on data shown in Figure 6, the concentration of $(NH_4)_2CO_3$ decreased from 3 mol/L to 1.9 mol/L after 1 h, and from 3 mol/L to 1.05 mol/L after 2 h.

The results of SEM-EDX analysis of precipitates produced in the process of REM ion-associates decay are illustrated in Figures 7 and 8 using thulium precipitate as an example. The thulium precipitate was composed of 71.48 wt. % thulium (Tm), 23.63 wt. % oxygen (O), and 4.89 wt. % carbon (C).

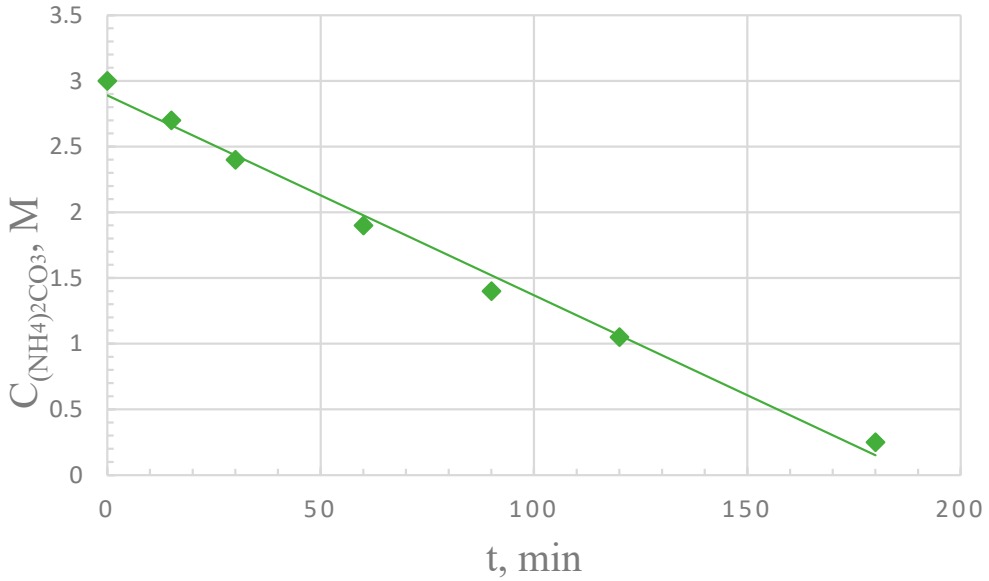

Figure 6. Kinetics of $(NH_4)_2CO_3$ decomposition.

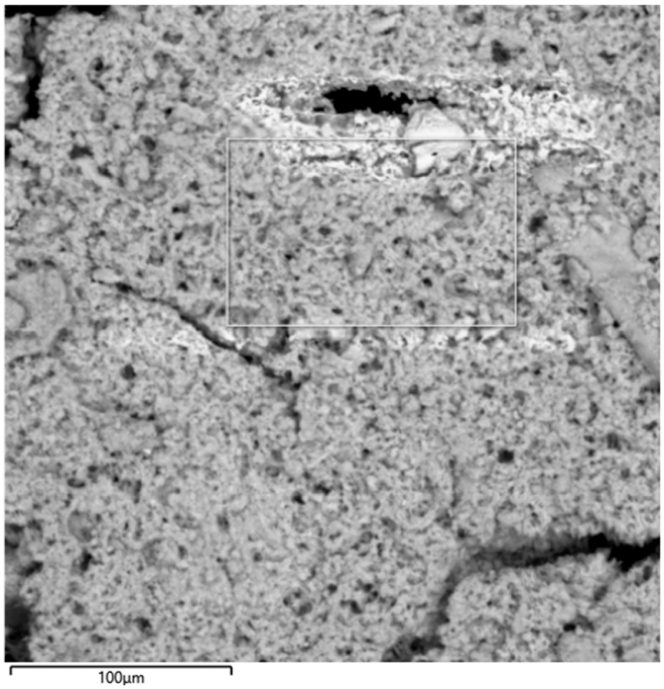

Figure 7. SEM image of thulium precipitate during its ion-associate decay.

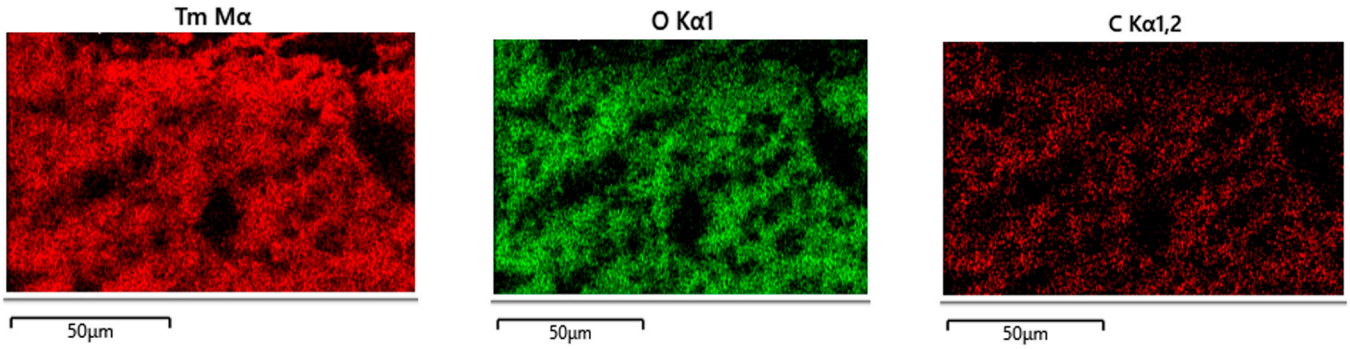

Figure 8. SEM-EDX mapping of thulium precipitate during its ion-associate decay.

Preliminary experiments in the field of REM leaching from technogenic phosphogypsum were carried out. Leaching was organized by a 4 M carbonate solution that was stirred for 3 h at a temperature of 90 °C and an L:S 100 mL per 1 g of PG. The degrees of extraction were as follows: La—40.1%, Ce—58.2%, Nd—62.5%, Dy—64.0%, Er—66.4%, Y—72.9%, and Yb—76.8%.

4. Discussion

The difference in cerium (III) carbonate solubility in potassium, sodium, and ammonium carbonate medium indicates the influence of the cation nature, which is characteristic of the association process.

The initial change in electrical conductivity, as shown in Figure 4, was caused by the formation of a suspension, with a higher amount of added powder (such as 0.1 g, 2 g, and 5 g) leading to a greater drop in the conductivity of the solution. After 2 min, an increase in specific electrical conductivity was observed, accompanied by the dissolution of $Tm_2(CO_3)_3$. Complete dissolution of the precipitate, depending on the solid-to-liquid ratio, was observed within 5–10 min. Complete dissolution of the precipitate was characterized by the return to the initial SEC value (263.2 mS/cm) for all considered phase ratios, confirming the formation of a thulium carbonate complex in the form of an ion-associate.

The behavior of carbonate complexes of light REEs (lanthanum and neodymium), medium-mass REEs (samarium and gadolinium), and heavy REEs (terbium, dysprosium, holmium, thulium, and yttrium) varied with a decrease in carbonate ion concentration. When heating solutions containing La (III), Nd (III), and Sm (III) at 70–75 °C, turbidity was observed at 15 min into the decomposition of ammonium carbonate, accompanied by the formation of the corresponding REE (III) carbonates. For Tb (III) and Dy (III), precipitation began at 20 min, for Ho (III) it began at 35 min, for Y at 40 min, for Tm at 110 min, and for Lu at 120 min.

According to the SEM-EDX analysis results, there was a possibility of the REM carbonate formation, or a like compound, in the ion-associate decay process. In a thulium carbonate, a mass fraction must be 65.24 wt. %, but it was in fact 71.48 wt. %. Therefore, the excursion was in the area of 6 wt. %

The tendency of REM carbonate complexes to decompose, forming a secondary precipitate such as $Ln_2(CO_3)_3$ upon a decrease in CO_3^{2-} concentration, serves as additional evidence that the soluble forms of Ln(III) in concentrated solutions of $(NH_4)_2CO_3$, K_2CO_3, or Na_2CO_3 are ion-associates.

Carbonate ion concentration decreases led to a chemical equilibrium shift towards the formation of REM carbonates. Moreover, the difference in the time required for the disintegration of ion-associates can be explained by the difference in individual elements' stability constants; i.e., a higher value of the stability constant required longer heating for a significant decrease in the carbonate ion in the solution.

The variation in the time required for the decay of ion-associates was due to differences in the strength of electrostatic attraction between anions and individual groups of REMs (III). Ions with a higher charge and smaller size exhibit stronger electrostatic interactions [40]. Therefore, the shorter decay times of light and medium REM associates resulted from their lower stability, indirectly suggesting a predominance of loose associates. In contrast, the strong associates formed by heavy REMs were primarily characterized as close (contact) associates.

The concentration of $(NH_4)_2CO_3$ in the productive solution after the decay of ion-associates was assumed to be according to Figure 6. An example of the material balance is presented in Table 2, characterizing the decay process of the terbium (III) ion-associate during heating for 1 h.

Table 2. Material balance of process for terbium carbonate formation.

Input			Output		
№	**Item**	**Mass, g**	**№**	**Item**	**Mass, g**
1	Ammonium carbonate solution: Ammonium carbonate Water	219.40 57.60 161.80	1	Productive solution: Ammonium carbonate Ammonium nitrate	199.00 34.10 0.96
2	Terbium nitrate (III) solution: Terbium nitrate (III) Water	11.18 1.38 9.8		Water	163.94
			2	Water Water (evaporation) Water from Equation (5)	11.06 6.55 4.51
			3	Ammonia	8.51
			4	Carbon dioxide	11.02
			5	Terbium carbonate (III)	0.99
	Total:	230.58		Total:	230.58

The material balance accounts for the processes described by Equations (8) and (12), which are end-to-end, and consist of Equations (5)–(11).

$$\text{Precipitation}: \ 2Ln^{3+}_{(aq)} + 3CO^{2-}_{3(aq)} \rightarrow Ln_2(CO_3)_{3(s)} \quad (5)$$

$$\text{Ion-association (dissolution)}: \ Ln_2(CO_3)_{3(s)} + CO^{2-}_{3(aq)} \rightarrow 2Ln(CO_3)^{-}_{2(aq)} \quad (6)$$

$$\text{Decay of ion-associates}: \ 2Ln(CO_3)^{-}_{2(aq)} \rightarrow Ln_2(CO_3)_{3(s)} + CO^{2-}_{3(aq)} \quad (7)$$

$$\text{End-to-end equation}: \ 2Ln^{3+}_{(aq)} + 3CO^{2-}_{3(aq)} \rightarrow Ln_2(CO_3)_{3(s)} \quad (8)$$

$$\text{Hydrolysis}: \ 2NH^{+}_{4(aq)} + CO^{2-}_{3(aq)} + 2H_2O_{(l)} \rightarrow 2NH_3{\cdot}H_2O_{(l)} + H_2CO_{3(l)} \quad (9)$$

$$\text{Decomposition}: \ H_2CO_{3(l)} \rightarrow CO_{2(g)} + H_2O_{(l)} \quad (10)$$

$$\text{Decomposition}: \ NH_3{\cdot}H_2O_{(l)} \rightarrow NH_{3(g)} + H_2O_{(l)} \quad (11)$$

$$\text{End-to-end equation}: \ 2NH^{+}_{4(aq)} + CO^{2-}_{3(aq)} \rightarrow 2NH_{3(g)} + CO_{2(g)} + H_2O_{(l)} \quad (12)$$

Figure 9 shows the calculated values of Gibbs energy for mono- and di-carbonate REM complexes in carbonate–carbonate systems. Similar values were obtained when REM sulfates and phosphates were leached by carbonate solution [41]. Therefore, complexation processes are possible.

If Ln is Tb, the Gibbs energy change at standard conditions during these processes as ΔG° (5) or (8) = −2.27 kJ/mol, ΔG° (6) ≈ −160 kJ/mol, and ΔG° (7) = 149.46 kJ/mol. The reactions from (9) to (12) are characterized as follows: ΔG° (9) = 230.70 kJ/mol, ΔG° (10) = −104.02 kJ/mol, ΔG° (11) = 0.28 kJ/mol, and ΔG° (12) = 127.24 kJ/mol.

On one hand, a positive value of ion-associate decay (7) reflects a theoretical stability of the complex compound. However, on the other hand, a carbonate ion decrease and its subsequent removal from the system lead to an equilibrium shift towards the REM carbonates' formation. This can be explained either by the formation of intermediate compounds or by complexation as an ion-association without strong covalent bonds.

Based on the analysis of the temperature effect at 60–75 °C on the decay of ion-associates (due to the decrease in ammonium carbonate concentration), the formation of rare earth metal (III) carbonates up to terbium occurred in a shorter time (τ_2) and with a higher yield compared to heavier rare earth metals, whose ion-associates decayed over a longer time (τ_1). Thus, the mechanism for the formation of rare earth metal (III) carbonates can be characterized by the scheme shown in Figure 10.

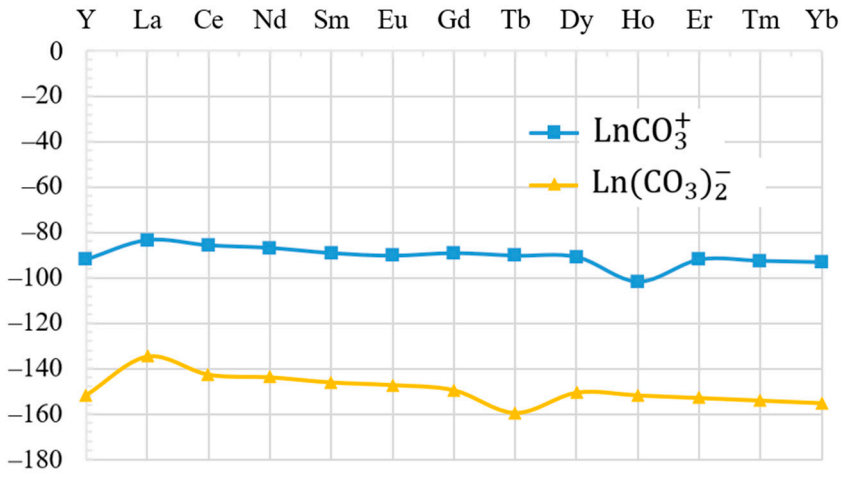

Figure 9. Gibbs energy changes during rare earth metal (III) carbonates' dissolution in carbonate-ion medium.

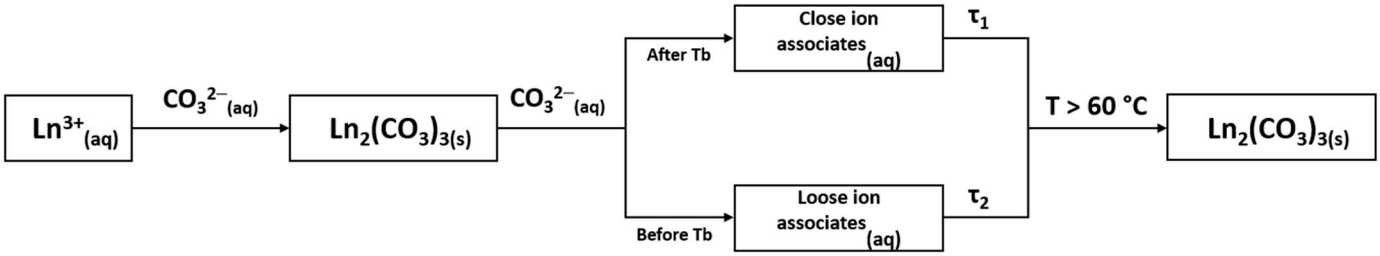

Figure 10. Mechanism of formation of rare earth metal (III) carbonates under atmospheric pressure.

5. Conclusions

These experimental findings confirm the existence of complex compounds of rare earth metals in the form of ion-associates within a high-concentration carbonate-ion medium (3 mol/L). The strength of electrostatic attraction between REM (III) ions and carbonate anions systematically increased from the light to the heavy REM group, which directly influenced the stability of the resulting associates. Ion-associates of light REMs and medium-mass REMs (up to terbium) were predominantly characterized as loose, whereas those formed by metals beyond terbium were more likely to be contact associates. Variations in the time required for REM (III) carbonates to precipitate resulted in distinct concentration thresholds for different REM groups. These observations suggest that during the carbonate–alkaline processing of primary or secondary REM sources into REM (III) carbonates, the formation of ion-associates as intermediate products may facilitate group separation of REMs through selective precipitation.

Particularly, phosphogypsum processing by the carbonate method should involve treatment of the solid phase by ammonium carbonate exclusively or a mixed ammonium and potassium (sodium) carbonates solution, depending on the REM content in the material. Because the vast majority of technogenic PG includes predominantly light REMs, the second variant would be more prospective. In this case, REM ion-associates needed insignificant carbonate ion decrease for decay into REM carbonates.

Author Contributions: Conceptualization, T.L. and S.G.; methodology, T.L.; software, V.S.; validation, V.S. and E.L.; formal analysis, S.G. and E.L.; investigation, S.G.; resources, V.S.; data curation, T.L.; writing—original draft preparation, S.G.; writing—review and editing, T.L. and S.G.; visualization, V.S.; supervision, T.L.; project administration, S.G. All authors have read and agreed to the published version of the manuscript.

Funding: This research received no external funding.

Data Availability Statement: The original contributions presented in this study are included in the article. Further inquiries can be directed to the corresponding author.

Conflicts of Interest: The authors declare no conflicts of interest.

References

1. Cherepovitsyn, A.; Solovyova, V.; Dmitrieva, D. New challenges for the sustainable development of the rare-earth metals sector in Russia: Transforming industrial policies. *Resour. Policy* **2023**, *81*, 103347. [CrossRef]
2. Cuadros-Muñoz, J.-R.; Jimber-del-Río, J.-A.; Sorhegui-Ortega, R.; Zea-De la Torre, M.; Vergara-Romero, A. Contribution of Rare Earth Elements Is Key to the Economy of the Future. *Land* **2024**, *13*, 1220. [CrossRef]
3. Pathapati, S.V.S.H.; Free, M.L.; Sarswat, P.K. A Comparative Study on Recent Developments for Individual Rare Earth Elements Separation. *Processes* **2023**, *11*, 2070. [CrossRef]
4. Leiva, C.; Arroyo-Torralvo, F.; Luna-Galiano, Y.; Villegas, R.; Vilches, L.F.; Fernández Pereira, C. Valorization of Bayer Red Mud in a Circular Economy Process: Valuable Metals Recovery and Further Brick Manufacture. *Processes* **2022**, *10*, 2367. [CrossRef]
5. Saidakhmetov, P.; Piyanzina, I.; Faskhutdinova, A.; Nedopekin, O.; Adyrbekova, G.; Baiman, G.; Suyerkulova, Z.; Romanova, I. Ab Initio Magnetic Properties Simulation of Nanoparticles Based on Rare Earth Trifluorides REF_3 (RE = Tb, Dy, Ho). *Crystals* **2023**, *13*, 1487. [CrossRef]
6. Castro, L.; Blázquez, M.L.; González, F.; Muñoz, J.Á. Biohydrometallurgy for Rare Earth Elements Recovery from Industrial Wastes. *Molecules* **2021**, *26*, 6200. [CrossRef]
7. Pirzada, M.D.S. Alternative Resources of Rare Earth Elements in Pakistan. *Mater. Proc.* **2024**, *17*, 26. [CrossRef]
8. Amirshahi, S.; Jorjani, E. Preliminary Flowsheet Development for Mixed Rare Earth Elements Production from Apatite Leaching Aqueous Solution Using Biosorption and Precipitation. *Minerals* **2023**, *13*, 909. [CrossRef]
9. Cook, N.J.; Ciobanu, C.L.; Wade, B.P.; Gilbert, S.E.; Alford, R. Mineralogy and Distribution of REE in Oxidised Ores of the Mount Weld Laterite Deposit, Western Australia. *Minerals* **2023**, *13*, 656. [CrossRef]
10. Mitrofanova, G.V.; Chernousenko, E.V.; Kompanchenko, A.A.; Kalugin, A.I. Specific action of collector from phosphoric acid alkyl esters class in flotation of apatite-nepheline ores. *J. Min. Inst.* **2024**, *268*, 637–645.
11. Skublov, S.G.; Levashova, E.V.; Mamykina, M.E.; Gusev, N.I.; Gusev, A.I. The polyphase Belokurikhinsky granite massif, Gorny Altai: Isotope-geochemical study of zircon. *J. Min. Inst.* **2024**, *268*, 552–575.
12. Pashkevich, M.A.; Danilov, A.S. Ecological security and sustainability. *J. Min. Inst.* **2023**, *260*, 153–154.
13. Ma, F.; Chen, L.; Lin, Z.; Liu, Z.; Zhang, W.; Guo, R. Microstructure and Key Properties of Phosphogypsum-Red Mud-Slag Composite Cementitious Materials. *Materials* **2022**, *15*, 6096. [CrossRef] [PubMed]
14. Prischepa, O.M.; Kireev, S.B.; Nefedov, Y.V.; Martynov, A.V.; Lutsky, D.S.; Krykova, T.N.; Sinitsa, N.; Xu, R. Theoretical and methodological approaches to identifying deep accumulations of oil and gas in oil and gas basins of the Russian Federation. *Front. Earth Sci.* **2023**, *11*, 1192051. [CrossRef]
15. Mukaba, J.-L.; Eze, C.P.; Pereao, O.; Petrik, L.F. Rare Earths' Recovery from Phosphogypsum: An Overview on Direct and Indirect Leaching Techniques. *Minerals* **2021**, *11*, 1051. [CrossRef]
16. Chernysh, Y.; Yakhnenko, O.; Chubur, V.; Roubík, H. Phosphogypsum Recycling: A Review of Environmental Issues, Current Trends, and Prospects. *Appl. Sci.* **2021**, *11*, 1575. [CrossRef]
17. Elbagory, M.; Shaker, E.M.; El-Nahrawy, S.; Omara, A.E.-D.; Khalifa, T.H. The Concurrent Application of Phosphogypsum and Modified Biochar as Soil Amendments Influence Sandy Soil Quality and Wheat Productivity. *Plants* **2024**, *13*, 1492. [CrossRef]
18. Guan, Q.; Sui, Y.; Liu, C.; Wang, Y.; Zeng, C.; Yu, W.; Gao, Z.; Zang, Z.; Chi, R.-a. Characterization and Leaching Kinetics of Rare Earth Elements from Phosphogypsum in Hydrochloric Acid. *Minerals* **2022**, *12*, 703. [CrossRef]
19. Ziying, C.; Zhan, L.; Jia, C.; Parashuram, K.; Fawzi, B.; Hongdeng, Q. Recent advances in selective separation technologies of rare earth elements: A review. *J. Environ. Chem. Eng.* **2022**, *10*, 107104.
20. Cheremisina, O.V.; Gorbacheva, A.A.; Balandinsky, D.A.; Luo, Y.; Ponomareva, M.A. Synergistic effect of a mixture of ethoxyphosphoric esters and sodium oleate in aqueous solutions. *Colloids Surf. A Physicochem. Eng. Asp.* **2024**, *685*, 133314. [CrossRef]
21. Pyagai, I.; Zubkova, O.; Babykin, R.; Toropchina, M.; Fediuk, R. Influence of Impurities on the Process of Obtaining Calcium Carbonate during the Processing of Phosphogypsum. *Materials* **2022**, *15*, 4335. [CrossRef] [PubMed]
22. Lutskiy, D.S.; Lukyantseva, E.S.; Mikheeva, V.Y.; Grigorieva, L.V. Investigation of the extraction of samarium and gadolinium from leaching solutions of phosphorus-containing raw materials using solid extractants. *Arab J. Basic Appl. Sci.* **2023**, *30*, 68–73. [CrossRef]
23. Millero, F.J.; Schreiber, D.R. Use of the ion pairing model to estimate activity coefficients of the ionic components of natural waters. *Am. J. Sci.* **1982**, *282*, 1508–1540. [CrossRef]

24. Byrne, R.H. Inorganic speciation of dissolved elements in seawater: The influence of pH on concentration ratios. *Geochem. Trans.* **2003**, *3*, 11–16. [CrossRef] [PubMed]
25. Sobolev, B.P.; Sulyanova, E.A. Lanthanide Contraction in LnF_3 (Ln = Ce-Lu) and Its Chemical and Structural Consequences: Part 2: Specialized Empirical System of R^{3+} (R = Y, La, and 14 Ln) and F^{1-} Ionic Radii for RF_3 Series. *Int. J. Mol. Sci.* **2023**, *24*, 17080. [CrossRef]
26. Sukhanova, K.G. Trace elements in the silicate minerals of the Borodino Meteorite (H5). *J. Min. Inst.* **2024**, *265*, 16–33.
27. Lan, Q.; Yang, Y.; Xie, Z.; Guo, H.; Liu, D.; Zhang, X. Molecular Dynamics Calculation of the Coordination Behavior of Yb (III) in Sodium Carbonate Solution. *Processes* **2023**, *11*, 2624. [CrossRef]
28. Surkova, A.; Bogomolov, A.; Paderina, A.; Khistiaeva, V.; Boichenko, E.; Grachova, E.; Kirsanov, D. Milk Analysis using a New Optical Multisensor System Based on Lanthanide (III) Complexes. *Eng. Proc.* **2023**, *48*, 28. [CrossRef]
29. Cantrell, K.; Byrne, R. Rare earth element complexation by carbonate and oxalate ions. *Geochim. Cosmochim. Acta* **1987**, *51*, 597–605. [CrossRef]
30. Lobacheva, O.L. Ion Flotation of Ytterbium Water-Salt Systems—An Innovative Aspect of the Modern Industry. *Water* **2021**, *13*, 3493. [CrossRef]
31. Firsching, F.; Mohammadzadei, J. Solubility products of the rare-earth carbonates. *J. Chem. Eng. Data* **1986**, *31*, 40–42. [CrossRef]
32. Ohta, A. Experimental and theoretical studies of REE partitioning between Fe hydroxide and Mn oxide and seawater. *Chikyukagaku (Geochem.)* **2006**, *40*, 13–30, (In Japanese with English abstract).
33. Olender, R.; Nitzan, A. Lattice theory of solvation and dissociation in macromolecular fluids. II. Quasichemical approximation. *J. Chem. Phys.* **1994**, *101*, 2338–2349. [CrossRef]
34. Finney, A.R.; Lectez, S.; Freeman, C.L.; Harding, J.H.; Stackhouse, S. Ion Association in Lanthanide Chloride Solutions. *Chem. A Eur. J.* **2019**, *25*, 8725–8740. [CrossRef] [PubMed]
35. Smolyakov, B.; Veselova, G. Limiting Equivalent Conductivities of Ions in Water Between 25 and 200 C. *Elektrokhim* **1975**, *11*, 700–704.
36. Ismail, I.M.; Masuko, Y.; Tomiyasu, H.; Fujii, Y. Conductivity of some rare earth chlorides in sub and supercritical aqueous solutions. *J. Supercrit. Fluids* **2003**, *25*, 69–79. [CrossRef]
37. Kellermeier, M.; Raiteri, P.; Berg, J.K.; Kempter, A.; Gale, J.D.; Gebauer, D. Entropy drives calcium carbonate ion association. *ChemPhysChem* **2016**, *17*, 3535–3541. [CrossRef]
38. Oleynik, I.L. Increasing the Processing Degree of Phosphate Raw Materials with the Associated Extraction of the Rare Earth Metals. The Dissertation Abstract for the Degree of Candidate of Technical Sciences. 2021. Available online: https://spmi.ru/sites/default/files/imci_images/sciens/dissertacii/2021/oleynik_avtoreferat.pdf (accessed on 17 February 2025).
39. Pawlowicz, R. Calculating the conductivity of natural waters. *Limnol. Oceanogr. Methods* **2008**, *6*, 489–501. [CrossRef]
40. Fang, Y. Ions Interacting with Macromolecules NMR Studies in Solution. Ph.D. Thesis, KTH Royal Institute of Technology, Stockholm, Sweden, 2017; p. 71.
41. Litvinova, T.E.; Oleinic, I.S.; Lutskiy, D.S. Thermodynamic justification of the extraction of rare-earth metals during the carbonate conversion of secondary phosphate raw materials. *ARPN J. Eng. Appl. Sci.* **2020**, *15*, 2919–2924.

Disclaimer/Publisher's Note: The statements, opinions and data contained in all publications are solely those of the individual author(s) and contributor(s) and not of MDPI and/or the editor(s). MDPI and/or the editor(s) disclaim responsibility for any injury to people or property resulting from any ideas, methods, instructions or products referred to in the content.